Journal of Nuclear Materials 386–388 (2009) 411–417

Contents lists available at ScienceDirect

Journal of Nuclear Materials

journal homepage: www.elsevier.com/locate/jnucmat

Recent progress toward development of reduced activation ferritic/martensitic steels for fusion structural applications

R.J. Kurtz [a,*], A. Alamo [b], E. Lucon [c], Q. Huang [d], S. Jitsukawa [e], A. Kimura [f], R.L. Klueh [g], G.R. Odette [h], C. Petersen [i], M.A. Sokolov [g], P. Spätig [j], J.-W. Rensman [k]

[a] Pacific Northwest National Laboratory, P.O. Box 999, Richland, WA 99352, USA
[b] CEA-Saclay, DEN/DSOE, Gif-sur-Yvette, France
[c] SCK-CEN, NMS, Mol, Belgium
[d] Institute of Plasma Physics, Chinese Academy of Sciences, Hefei, Anhui 230031, China
[e] Japan Atomic Energy Agency, Tokyo, Japan
[f] Kyoto University, Kyoto, Japan
[g] Oak Ridge National Laboratory, Oak Ridge, TN, USA
[h] University of California at Santa Barbara, Santa Barbara, CA, USA
[i] FZK-IMF, Karlsruhe, Germany
[j] Fusion Technology-Materials, CRPP EPFL, Association EURATOM-Confédération Suisse, 5232 Villigen PSI, Switzerland
[k] NRG, Petten, The Netherlands

ARTICLE INFO

PACS:
F0800
S1000
S1100

ABSTRACT

Significant progress has been achieved in the international research effort on reduced activation ferritic/martensitic steels for fusion structural applications. Because this class of steels is the leading structural material for test blankets in ITER and future fusion power systems, the range of ongoing research activities is extremely broad. Since, it is not possible to discuss all relevant work in this brief review, the objective of this paper is to highlight significant issues that have received recent attention. These include: (1) efforts to measure and understand radiation-induced hardening and embrittlement at temperatures $\leqslant$400 °C, (2) experiments and modeling to characterize the effects of He on microstructural evolution and mechanical properties, (3) exploration of approaches for increasing the high-temperature (>550 °C) creep resistance by introduction of a high-density of nanometer scale dispersoids or precipitates in the microstructure, (4) progress toward structural design criteria to account for loading conditions involving both creep and fatigue, and (5) development of nondestructive examination methods for flaw detection and evaluation.

1. Introduction

Reduced-activation ferritic/martensitic (RAF/M) steels with a nominal composition of Fe–0.1C–9Cr–2W–0.25V–0.07Ta are the reference first-wall and blanket structural material for both ITER test blanket modules and future fusion power systems in essentially all of the worldwide fusion materials research programs. RAF/M steels are attractive for fusion applications because of their high-level of technological maturity relative to low-activation alternatives, such as vanadium alloys and SiC composites [1–3]. Initial experience with ferritic/martensitic steels was gained in high-flux fast reactor development programs before reduced activation versions were considered as structural materials for fusion. Advantages of these steels include: (1) a well-developed technology for nuclear and other advanced technology applications, (2) resistance to radiation-induced swelling and He embrittlement, and (3) compatibility with aqueous, gaseous, and liquid metal coolants which allows for many design options. While considerable progress has been made in recent years, there are a number of critical issues that must be resolved before successful application in a fusion power system can be achieved. The effects of radiation-induced hardening and embrittlement at low-temperatures need to be better-characterized, particularly non-hardening embrittlement mechanisms. Perhaps the overarching issue is the effect of high levels of transmutation-produced He on low-temperature fracture toughness and creep-rupture behavior at high temperature. Lacking experimental facilities to explore the effects of fusion relevant He and He/dpa ratios on mechanical properties has motivated fusion materials researchers to seek answers through a combination of innovative experiments and modeling. Extending the upper operating temperature limit to beyond ~550 °C and development of structural design criteria to account for creep-fatigue loading conditions are critical needs. Finally, the development of qualified

* Corresponding author. Tel.: +1 509 373 7515; fax: +1 509 376 0418.
E-mail address: rj.kurtz@pnl.gov (R.J. Kurtz).

0022-3115/$ - see front matter © 2009 Elsevier B.V. All rights reserved.
doi:10.1016/j.jnucmat.2008.12.323

nondestructive examination methods for flaw detection and evaluation in a geometrically complex system involving dissimilar materials and a wide range of fabrication and joining methods remains an important issue that has received only limited attention.

2. Hardening and embrittlement

Radiation-induced hardening and embrittlement in RAF/M steels has been extensively studied at temperatures ⩽500 °C. Below an irradiation temperature of ~400 °C, these steels harden considerably resulting in loss of ductility, an increase in the ductile-to-brittle-transition-temperature (DBTT) and loss of fracture toughness. Recent research has focused on assessing the effects of neutron irradiation on tensile properties [4–9]. Yamamoto et al. [4] have demonstrated that the dose dependence of the yield strength increase is effectively modeled by the following equation, which was first derived by Whapman and Makin [10]:

$$\Delta\sigma_y = \Delta\sigma_{ys}[1 - \exp(-\mathrm{dpa}/\mathrm{dpa}_0)]^p \quad (1)$$

where $\Delta\sigma_y$ is the yield strength change, $\Delta\sigma_{ys}$ is a saturation-hardening, dpa_0 specifies the dose transient prior to saturation, and p is an effective dispersed barrier hardening exponent assumed to have a value of ~1/2.

Fig. 1 shows data obtained by Lucon and Vandermeulen [5,6] and Petersen [7] on the effects of neutron irradiation on hardening of Eurofer97 over the temperature range 300–336 °C up to a dose of 69 dpa. The saturation-hardening dose for this steel in this temperature regime is about 10 dpa. The recently acquired high-dose data point confirms there is little increase in hardening beyond 10 dpa. Restricting the fit of Eq. (1) to just the 300 °C data results in a model that over predicts the saturation-hardening level relative to a fit that includes the higher dose data obtained at a somewhat higher irradiation temperature. The slope of the curve at low dpa characterizes the initial rate of hardening

$$k = \Delta\sigma_{ys}/\sqrt{\mathrm{dpa}_0} \quad (2)$$

where k is known as the hardening coefficient. Fig. 2 shows the temperature dependence of the hardening coefficient for RAF/M steels irradiated by both neutrons [4,8] and protons [9]. This plot clearly

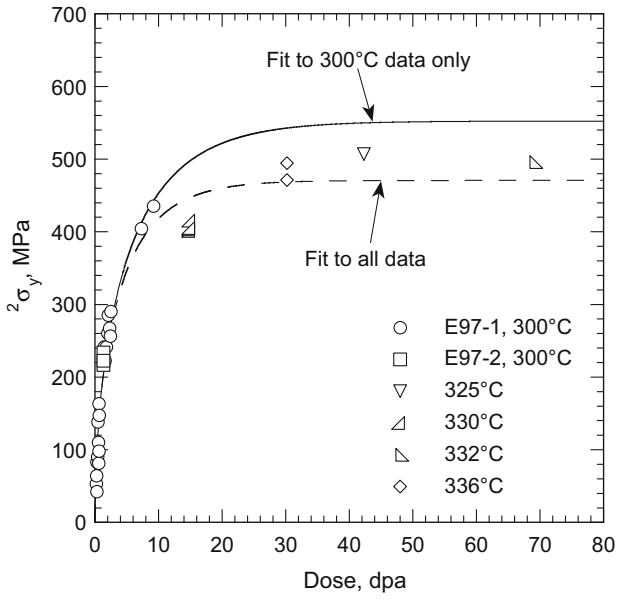

Fig. 1. Dose dependence of irradiation-induced yield stress increase for Eurofer97 with $T_{test} \sim T_{irr}$ [5–7].

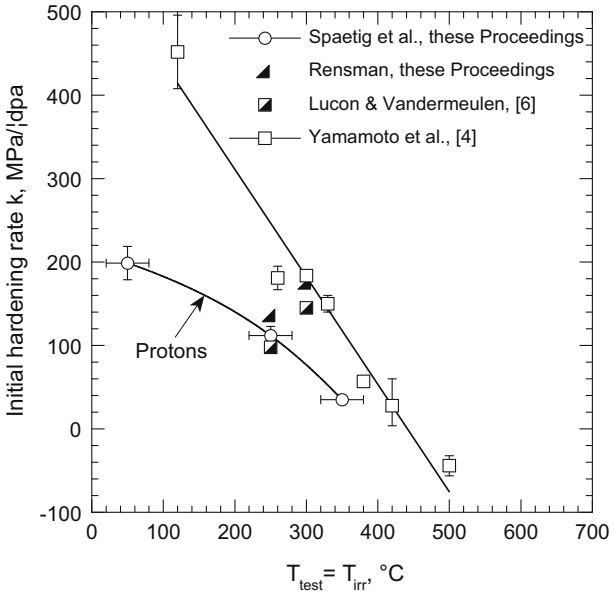

Fig. 2. Temperature dependence of the initial hardening coefficient for neutron and proton irradiated tempered martensitic steels with $T_{test} = T_{irr}$ [4–6,8,9].

demonstrates that hardening vanishes at irradiation temperatures above ~440 °C and softening is observed at 500 °C. While Yamamoto et al. chose to fit the data with a straight line the data point at ~250 °C clearly deviates from this trend.

To study the hardening rate behavior in more detail, a 9%Cr steel irradiation experiment called SUMO-09 was performed at irradiation temperatures of 250 and 300 °C [8]. Combined with data from previous irradiation experiments at these temperatures the new data confirms the lower hardening rate at 250 °C. The data points from Lucon and Vandermeulen [5,6] also confirm this result. It is interesting to note that initial hardening induced by protons follows a different trend at low-temperatures [9] but appears to converge with the neutron data at temperatures above ~300 °C.

Several forms of irradiation-induced embrittlement have been identified in RAF/M steels. Perhaps the most extensively studied is embrittlement associated with irradiation hardening. The Master Curve (MC) – shifts method can be used to quantitatively model hardening-induced embrittlement that results in increases in the cleavage transition fracture toughness reference temperature (ΔT_0) [11]. Recent MC research has concentrated on determining if the MC has a universal shape and the physical basis for the method. While it is traditional to relate ΔT_0 to corresponding changes in yield stress, $\Delta\sigma_y$, as $C_0 = \Delta T_0/\Delta\sigma_y$, recent research [12] has established that it is the strain-hardened flow stress, $\Delta\sigma_{fl}$, in the fracture process zone that controls cleavage, rather than the yield stress. Thus, irradiation-induced decreases in strain hardening need to be considered along with yield stress increases in evaluating ΔT_0.

Odette et al. [12] proposed a simple model for small scale yielding conditions in which cleavage occurs when a critical volume of material, V^*, ahead of a crack tip experiences a critical stress, σ^*, normal to the crack plane. Given the temperature dependences of σ^* and σ_y the shape of the MC can be accurately predicted. Finite element simulations were performed to assess the effect of a realistic range of true stress – true strain behaviors indicative of RAF/M steels irradiated at low-temperatures and low-doses. Under these irradiation conditions as yield stress increases there is a corresponding loss of strain-hardening capacity. The calculated MCs showed that reduced strain-hardening capacity decreases ΔT_0, partially offsetting the increase associated with $\Delta\sigma_y$. Thus, C_0 is lower for steels that exhibit loss of strain-hardening capacity. A second

important finding from their work is that it is possible to derive a universal relation between ΔT_0 and $\Delta\sigma_{fl}$ averaged over a pertinent range of true strain. Their results showed that $\Delta\sigma_{fl}$ averaged from ε 0 to 0.1 provided a similar C_0, for various assumptions about the effect of irradiation on strain-hardening capacity.

Mueller et al. [13] explored the fracture toughness behavior of Eurofer97 steel in the lower to middle ductile-to-brittle transition region. The results of their analysis showed that in the lower transition region the ASTM E1921 MC did not satisfactorily predict the median toughness and associated scatter. To improve the description of the data near the lower shelf region, two parameters of the MC, namely the thermal component, A, and the reference temperature, T_0 were fitted by the maximum likelihood method. An A value of 12.2 MPa $m^{1/2}$ produced the best fit to the data, but this value is significantly lower than the ASTM recommended value of 30 MPa $m^{1/2}$. The modified MC permitted accurate determination of T_0 from tests performed at temperatures near the lower shelf toughness. In fact, the value of T_0 was independent of the dataset used to determine it when using the single temperature method. A conclusion from the work of Mueller et al. is that with moderate MC shape adjustments, it is possible to extend the MC from the transition region down to temperatures below that recommended in the ASTM standard. Such shape adjustments may make it feasible to determine T_0 from small specimens tested near the lower shelf.

While hardening and embrittlement associated with displacement damage are perhaps the predominant factors controlling the lower operating temperature limit for RAF/M steels, non-hardening embrittlement (NHE) phenomena may play a significant role in controlling the strength and toughness of these steels at operating temperatures $\geqslant$450 °C. Potential NHE phenomena include: (1) precipitation and coarsening of brittle phases that trigger cleavage or intergranular fracture, (2) segregation at grain boundaries of trace elements such as P or depletion of beneficial elements like C, (3) instabilities in the dislocation or lath-packet substructures leading to larger effective subgrain sizes, and (4) grain boundary decohesion due to microcracks, gas bubbles (He and H), and creep cavities. Yamamoto et al. [4] compiled the limited data on thermal embrittlement of RAF/M steels and concluded that transition temperature shifts of up to ~90 °C are observed when these steels are aged in the temperature range from 500 to 650 °C for times less than 10 000 h. The NHE due to thermal aging is thought to be due to precipitation of brittle Laves phases on the grain boundaries [4].

A recent analysis by Klueh et al. [14] demonstrated that embrittlement can occur in RAF/M steels at temperatures >425 °C, where little or no irradiation hardening is found. Aging data on F82H steel showing embrittlement but no hardening after 30 000 h at temperatures between 500 to 650 °C were analyzed by performing thermodynamic calculations. The DBTT increased 105 °C and the room temperature yield stress decreased 180 MPa after 30 000 h at 650 °C. The result of their analysis is presented in Fig. 3 in which the amount of extracted precipitates from aged specimens are compared to calculated amounts of $M_{23}C_6$ and Laves precipitates. Their results show that $M_{23}C_6$ is largely formed during tempering at 750 °C, and little more of this precipitate forms by aging between 400 and 650 °C. The potential for relatively large amounts of Laves exists at 400 °C and decreases as the aging temperature increases. Note that equilibrium is achieved in 30 000 h at 650 °C as the total estimated precipitate amount closely matches the amount measured from the extraction experiment. A conclusion from their work is that the thermal embrittlement of F82H is due to Laves precipitation and that this process could be accelerated by neutron irradiation. As an example of such embrittlement, the authors cite the work of Sokolov et al. who found embrittlement of F82H irradiated in HFIR at 500 °C due to Laves phase. The embrittlement occurred despite a decrease in yield stress [15]. Consequently there is a need for high-dose irradiation experiments above the irradiation-hardening regime [14].

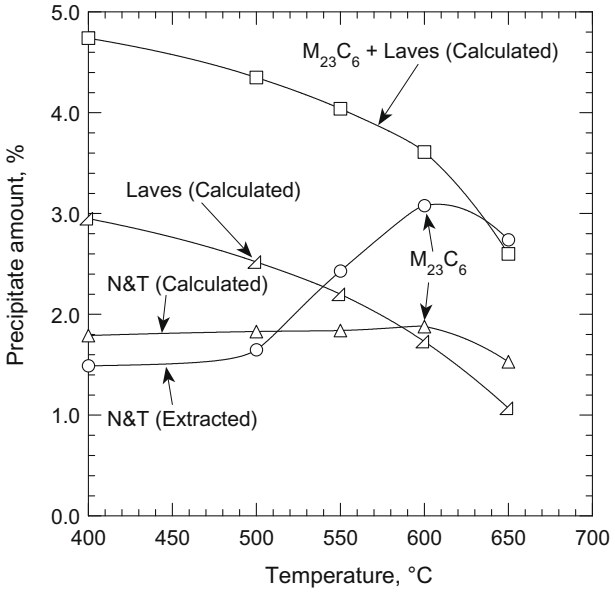

Fig. 3. Temperature dependence of the amount of precipitate formed in unirradiated F82H. The two major precipitates formed are $M_{23}C_6$ and Laves. The JMatPro code was used to obtain the calculated values. Note that most of the $M_{23}C_6$ is formed during tempering at 750 °C as the amount that forms between 400 and 650 °C is relatively constant. The amount of Laves precipitate decreases as the temperature increases. Experimental measurement of $M_{23}C_6$ amount was obtained by extraction. Note equilibrium is achieved in 30 000 h at 650 °C [14]. N&T, normalized-and-tempered.

3. Helium effects experiments and modeling

Accumulation of He can have major consequences for the integrity of fusion structures such as loss of high-temperature creep strength, increased swelling and irradiation creep at intermediate temperatures, and the potential for loss of ductility and fracture toughness at low-temperatures. Helium is essentially insoluble in metals and strongly interacts with and binds to numerous microstructural features. After more than ~40 years of research on He effects there remain a number of key questions that have not been resolved. Examples include: (1) what is the sequence of events that controls the fate of He once it is generated, (2) how does He diffuse, (3) how and where is He trapped, (4) what processes control He bubble nucleation, and (5) how does the type of sink affect He bubble density and size? In a key set of experiments performed about 25 years ago, Schroeder and Batfalsky [16] demonstrated that the manner in which He is introduced into the microstructure can drastically alter its effects on mechanical properties. The creep-rupture lifetime of specimens pre-implanted with 100 appm He was orders of magnitude larger than 'in-beam' specimens in which He was injected at 100 appm/h while under load.

A standard method for characterizing the effect of He on hardening and embrittlement is to determine ductile-to-brittle transition temperature shifts from Charpy impact tests, ΔT_c, and plot that information against the corresponding change in yield strength, $\Delta\sigma_y$. For RAF/M steels in the absence of He, such a plot gives a linear correlation with a slope, $C_c = \Delta T_c/\Delta\sigma_y$, that range from 0.20 to 0.56 °C/MPa for irradiation temperatures below 400 °C [4]. Generally, at low concentrations, the effect of He is to incrementally harden and embrittle a material similar to that produced by displacement damage. There are several possible effects

He can have on mechanical properties. Helium could stabilize vacancy clusters causing an increase in the number of interstitial clusters that eventually form dislocations that increase strength, or He could simply stabilize clusters to higher temperatures. Helium could diffuse to grain boundaries and induce intergranular fracture. A large number of He filled bubbles could form thereby increasing resistance to dislocation motion. Recent analyses by Yamamoto et al. [4] and Klueh et al. [17,18] suggest that He may play a role in NHE. In these analyses large increases in C_c with increasing He content, as well as a transition from transgranular cleavage to intergranular fracture, were interpreted as signatures of a possible NHE due to He. While the data is scattered or may be confounded by uncontrolled variables, the results indicate that He has little effect on C_c or ΔT_c until concentrations of several hundred appm are reached [4].

It is difficult to explore the effects of He under prototypic conditions due to a lack of appropriate irradiation facilities. To design, develop and validate He resistant microstructures, appropriate experimental methods are needed to introduce He into a material at fusion relevant He-to-dpa ratios. Some methods for producing He in ferritic alloys such as B and Ni doping cause undesirable effects since the composition of the alloy is changed, potentially leading to the formation of atypical phases during irradiation. Isotopic tailoring of ferritic alloys with ^{54}Fe is an attractive approach for simulating He effects in Fe-based materials, but ^{54}Fe is costly and ultimately does not produce the correct He-to-dpa ratio.

An alternative method that avoids the limitations of the above approaches is application of a surface layer that under neutron irradiation injects He into the adjacent material [19]. A Ni bearing coating on any substrate causes production of energetic He atoms due to a two-step thermal neutron reaction sequence under mixed spectrum neutron irradiation conditions, and the He is injected into the substrate. With this approach it is possible to explore the effects of He on microstructural development by implanting He at almost any desired He-to-dpa ratio to a uniform depth of a few microns. It is not possible to obtain bulk mechanical property information by this technique, so it does not eliminate the need for a fusion-like intense neutron source. Fig. 4 gives two examples of the microstructures that are obtained by this technique. Fig. 4(a) shows a TEM image of F82H and Fig. 4(b) displays similar image for MA957, an oxide dispersion strengthened steel. Both specimens were irradiated at 500 °C in the High Flux Isotope Reactor to about 9 dpa and 380 appm He. Preliminary analysis of these images indicates that the bubble density in F82H ($\sim 1 \times 10^{23}/m^3$) is about a factor of three smaller than in MA957 ($\sim 3 \times 10^{23}/m^3$). The mean bubble radius is larger in F82H ($\sim$2 nm) than in MA957 ($\leqslant$1 nm). There is also evidence of polyhedral void formation in the F82H, but not in MA957. Cold worked F82H had a slightly higher density of smaller bubbles than annealed F82H. The bubbles are generally smaller and more numerous in F82H than found in Eurofer97 [19]. The bubbles in F82H are predominantly associated with dislocations and interfaces. These studies are just getting underway and will emphasize quantitative characterization of the irradiated microstructures, including additional alloys and irradiation conditions.

Computational modeling is an important tool for interpreting experiments and elucidating the mechanisms of He transport and fate in RAF/M steels. There have been significant recent efforts to model He effects over a broad spectrum of spatial and temporal scales. Electronic structure calculations indicate that interstitial He diffuses rapidly and binds with a wide range of vacancy and interstitial type point defects [20]. These calculations also show that tetrahedral interstitial He is more stable than octahedral interstitial He [20,21]. New semi-empirical Fe–He interatomic potentials have been developed that more accurately reproduce the *ab initio* interstitial and substitutional He formation energies in Fe [22]. Molecular statics and dynamics results using these new potentials compare favorably with the *ab initio* results and indicate a wide range of He binding energies with various microstructural defects [23–25]. Recent kinetic Monte Carlo simulations illustrate that He_nV_m clusters have high diffusivity in a Fe matrix [26,27].

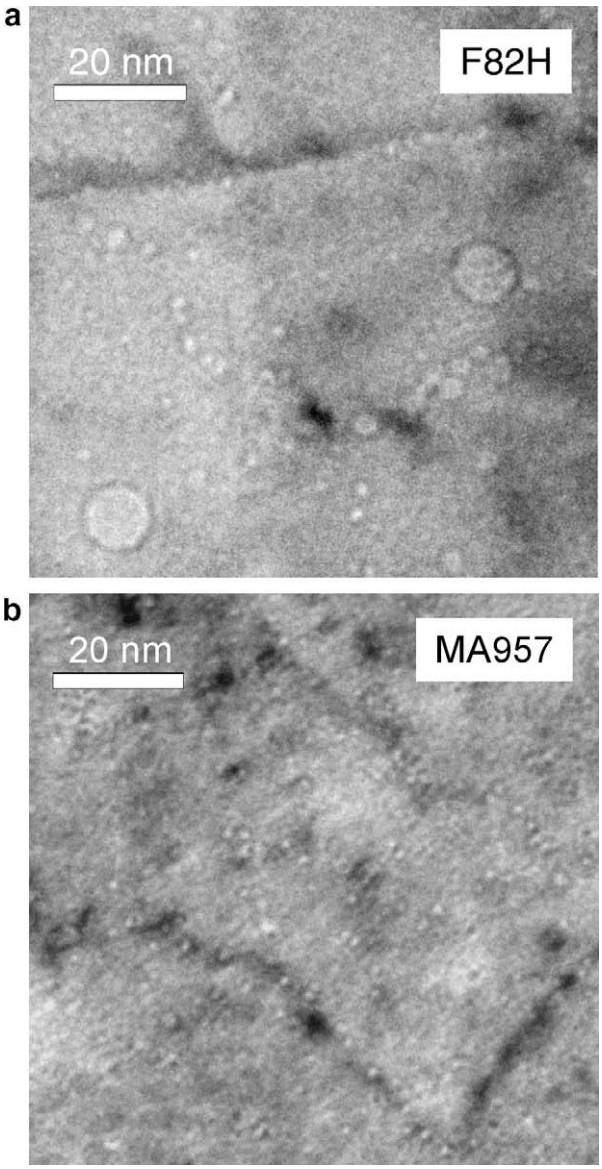

Fig. 4. Bubble and cavity microstructures for F82H (a), and MA957 (b) neutron irradiated in the HFIR at 500 °C to about 9 dpa and 380 appm He. Note that the mean bubble size is larger and number density smaller in F82H compared to MA957.

A recent paper by Schäublin and Chiu [28] illustrates the utility of computational modeling to explore how He bubbles can strengthen a material by blocking dislocation motion. They carried out molecular dynamics simulations of edge dislocation mobility in Fe to study the effect of He either as a gas in solid solution or in cavities. Their results showed that He in solid solution up to 1 at.% had little effect on the mobility of the edge dislocation. On the other hand, a 2 nm void and a 2 nm sessile a_0 [1 0 0] dislocation loop were strong obstacles with strengths of 590 MPa and 440 MPa, respectively. A 2 nm He bubble was found to be a weaker obstacle than the 2 nm void when the He-to-vacancy ratio was between one and two. At higher He-to-vacancy ratios, the resistance of the He bubble increased until at a He-to-vacancy ratio of five the

bubble was considerably stronger than a void, which was attributed to loop punching.

4. High-temperature creep resistance

The high-temperature strength of RAF/M steels is limited by its microstructural stability. At high-temperature $M_{23}C_6$ particles coarsen and the subgrain size increases. One approach to improving high-temperature strength is by introducing a high number density of stable, fine-scale, precipitates or dispersoids that interfere with the motion of dislocations. Considerable progress has been made on development of oxide dispersion strengthened (ODS) ferritic steels or nano-structured ferritic alloys (NFA) that are produced by powder metallurgical mechanical alloying methods. An advantage to this material design strategy is the creation of a radiation tolerant material by introduction of very high sink densities that trap transmutation-produced gases and provide sites for recombination of vacancies and self-interstitials. Thus, displacement damage is mitigated and the grain boundaries are shielded from accumulation of deleterious concentrations of He.

A detailed description of recent ODS/NFA development activities is given in a paper by Odette et al. [29], so only a few salient highlights will be presented here. The bulk of the research on ODS/NFA is being performed in the European Union (EU), Japan and the United States. In the EU, there is an effort underway to develop an ODS version of Eurofer [30]. The focus of this research is on optimizing the processing conditions, improving the DBTT, exploring the thermal creep resistance and characterizing the microstructure. Also in the EU there is research on 12–18Cr ODS ferritic alloys with an emphasis on understanding the role Ti plays in formation of the ~3 nm diameter Ti–Y–O nanoclusters. In Japan a similar effort is being carried out to develop 9Cr and 12Cr ODS steels for use as fuel cladding in advanced fission reactors. This work includes assessment of mechanical properties, particularly creep-rupture lifetimes in air and liquid Na, and extensive characterization of irradiation effects. Recent research in the US has focused primarily on the effects of low-dose neutron irradiation on tensile and fracture properties of a 1 kg heat of a 14Cr NFA (Fe–14Cr–3 W–0.4Ti + $0.3Y_2O_3$), the long-term stability of Ti–Y–O nanoclusters in MA957 and characterization of MA957 after neutron irradiation and simultaneous He injection to about 9 dpa at 500 °C.

Another approach to producing a creep-resistant microstructure is through novel thermo-mechanical treatments (TMT). This idea was proposed by de Carlan et al. [31] and independently by Klueh et al. [32] and the latter researchers applied the concept to commercial and experimental steel compositions. Thermodynamic calculations are performed to determine appropriate adjustments to the RAF/M steel composition to achieve a high number density of nanometer scale nitride (MX) precipitates. The basic TMT involves dissolving solutes in a temperature range between 1100 and 1300 °C, hot working between 750 and 1000 °C to introduce a dislocation substructure to provide sites for heterogeneous nucleation of MX precipitates, annealing to grow the precipitates to optimal size and finally an air cool to form the martensitic phase.

Recent results by Klueh [33] are shown in Fig. 5, which shows a plot of yield stress versus temperature for 9Cr–1MoVNbN steel in the normalized-and-tempered (N&T) condition and after two TMTs. The difference in the two is due to a difference in TMTs, showing optimization of the TMT process. There are also curves for 9Cr–1.8W–0.8MoVNbNB steel after N&T and TMT. For comparison, tensile data for the ODS 12YWT steel are shown. While the short-time tensile properties of nitride strengthened steels compare favorably with an ODS steel, it should not be inferred that

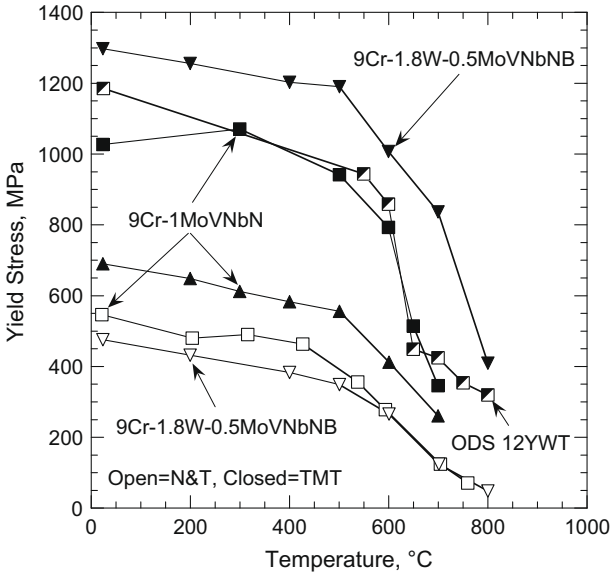

Fig. 5. Temperature dependence of the yield stress for unirradiated tempered martensitic steels in the normalized and tempered (N&T) condition compared to the same steels given a thermo-mechanical treatment (TMT) to produce a nanoscale nitride dispersion. An oxide dispersion strengthened (ODS) steel 12YWT is shown for comparison to the nitride strengthened steels [33].

the advanced TMTs described here will allow production of steels with upper service temperatures as high as ODS steels since nitrides are not as stable as oxides. Upper service temperatures in the range 650–700 °C may be achievable with nitride strengthened steels while avoiding the complexity of mechanical alloying needed for ODS alloys.

5. Structural design criteria

Structural elements of fusion power systems will be subjected to complex thermo-mechanical loading and high radiation doses that will induce both mechanical and irradiation damage. During service both types of damage occur concurrently resulting in significant property changes. There is a possibility of synergistic interactions, so damage evolution models based solely on separate effects experiments may not fully describe the observed changes. In addition, existing structural design codes for nuclear service do not apply to situations where large property changes occur. Consequently, current codes and standards will need to be modified or adapted to account for conditions unique to the fusion nuclear environment [34,35].

The development of test blanket modules (TBM) for ITER has stimulated interest in design criteria and qualification requirements for materials, structures and components. All of the ITER parties are developing blanket concepts that use RAF/M steels as the structural material [36], and a key requirement for testing a blanket concept in ITER is 'DEMO relevancy'. Thus, the TBM design, materials selection, and fabrication technology must be relevant to a DEMO-type fusion power system.

Salavy et al. [37] summarized the design features and fabrication technologies currently envisioned for the EU TBMs. Fabrication of subcomponents will involve numerous joining methods such as hot isostatic pressing that have not been qualified for nuclear service [37]. In addition, a variety of welding methods will be used to assemble the TBM box from the different subcomponents, and existing code rules govern only a few of the proposed welding configurations [37]. Several post-weld heat treatments will likely be needed during the assembly process, which

introduces additional microstructural variability. While the detailed fabrication techniques for TBMs being proposed by other parties differ from the EU approach, there are substantial similarities, so qualification of these techniques is essentially common to all. The EU has carried out an extensive review of the requirements to qualify TBM materials and fabrication technologies and concluded that a large validation program will be needed to define an appropriate and complete set of design and manufacturing criteria. In addition, a number of code cases will be needed to supply missing information on design criteria, material property data, fabrication technologies, and nondestructive inspection techniques and procedures.

The majority of lifetime prediction approaches and existing design criteria are typically based on data generated under uniaxial loading conditions at constant temperature [38]. A major effort to characterize and model creep-fatigue-oxidation interactions in 9Cr–1Mo martensitic steel has been reported by Fournier et al. [39–41]. The focus of that work was to develop lifetime prediction data and models based on a thorough understanding of the physical phenomena governing material behavior under uniaxial stress-relaxation and creep-fatigue loading conditions, including the perturbing effects of oxidation. Studies have also been performed to understand long-term microstructural development under creep-fatigue loading conditions [42–44]. During service structural components will experience both multiaxial loading and variable temperatures, so lifetime prediction methods and design criteria must be able to conservatively account for these conditions. In a recent study, Sunyk and Aktaa [45] evaluated some important design rules based on linear elastic simulations and compared their predictions to results of cyclic simulations of TBM behavior using advanced materials models that incorporate the cyclic softening characteristics of Eurofer97. Their results demonstrated that none of the design criteria were met. The selected design rules predicted plastic collapse and plastic instability as well as the probable accumulation of plastic deformation. The results of the cyclic simulation show neither plastic collapse nor ratcheting after 600 cycles. The difference suggests that the design criteria may be too conservative for Eurofer97.

In another investigation Aktaa et al. [38] performed thermo-mechanical and multiaxial fatigue tests on Eurofer97 specimens and compared the results to lifetime predictions based on fatigue life design rules derived from isothermal uniaxial data. They found that the design curves, despite inclusion of high safety factors, were not sufficiently conservative. They concluded that thermo-mechanical cycling of Eurofer97 produced more fatigue damage than isothermal fatigue cycling with the same mechanical strain range. Reduced cyclic softening under thermo-mechanical and isothermal multiaxial fatigue loading was identified as the principal reason for the much lower fatigue lifetimes observed under these loading conditions when compared to lifetimes achieved under uniaxial loading conditions.

While it is important to perform experiments that yield information on possible synergistic effects, it is surely not feasible to fully qualify materials and fabrication technologies solely by constructing an extensive database. The requirements for licensing DEMO and commercial power systems are not presently known, but it is anticipated that licensing authorities could rely on national codes, such as ASME. In this case, data on multiple heats and multiple product forms will be required. Fission reactor experience suggests that large test matrices will be needed to evaluate the effects of neutron irradiation on properties. Given the limited irradiation volume available in projected facilities such as IFMIF, this could present a challenge. In a recent IEA sponsored symposium on fusion reactor materials development [34], it was concluded that computational materials science is an indispensable tool for reducing the needed experimentation and optimally utilizing high-value facilities such as IFMIF.

6. Nondestructive evaluation

First-wall/blanket structures of fusion power systems will be geometrically complex, will be constructed from a wide variety of materials and will contain a considerable quantity of joined and bonded materials. A variety of techniques are under investigation for joining the RAF/M steel structural elements of ITER TBMs. These techniques include hot isostatic pressing (HIP), electron beam welding, laser welding, and tungsten inert gas welding [46]. Failures in engineered structures occur predominantly at welds and in weld heat affected zones [47], so it is imperative to minimize the incidence of weld defects during fabrication and post-weld heat treatments. Implementation of effective nondestructive examination (NDE) techniques and procedures is essential to ensure the safe and reliable operation of fusion power system structures and components.

A truly effective inspection program requires close integration of advanced structural analysis methods, fracture mechanics and NDE to develop the appropriate structural loading limits, flaw evaluation methods and flaw acceptance criteria. A single NDE technique will not be able to detect and size all flaws of interest due fundamental physics and human factors. Most likely a suite of NDE techniques and procedures will be needed to effectively inspect the large volume of welded and bonded material. A number of studies have been performed to assess the efficiency of several NDE techniques to detect and size defects in various components for ITER [48–53] and work is underway in the EU to develop the necessary inspection methods for TBM. It is imperative that such work focuses on detection and sizing of realistic flaws that could occur during fabrication and operation of mockups and components manufactured with the technologies to be used for commercial production of fusion power systems.

7. Near term issues for further research

While considerable progress has been made toward development of RAF/M steels for fusion applications there remain a number of issues that require further research to fully resolve. The MC – shifts method for characterizing embrittlement associated with microstructural changes due to radiation damage has been highly successful, but the fundamental validity and physical basis for the method is only beginning to be established. Further work is needed to verify that a universal MC shape exists. Size and geometry effects for shallow cracks remains to be resolved, as well as embrittlement due to synergistic hardening and NHE mechanisms caused by the effects of copious quantities of He and H.

Recent work on ODS/NFA has demonstrated that these materials exhibit significant potential as high-performance, radiation resistant alloys capable of managing displacement damage transmutant gas. The attractiveness of these materials would be enhanced if more cost-effective manufacturing methods could be developed, and joining technologies are needed that produce joints with properties similar to those of the base material. Another issue with ODS/NFA materials may be compatibility with coolants at higher operating temperatures. Success at expanding the upper operating temperature window to $\sim$800 °C could introduce corrosion problems with coolants such as PbLi.

Another topic requiring increased attention is high-temperature creep and creep-rupture, including the effects of high levels of He on these deformation processes. This is obviously a difficult topic to explore fully due to lack of facilities for introducing He in a prototypic manner, but progress is possible by combining innovative

experiments and advanced computational modeling methods. Related to this topic is the issue of creep-fatigue interaction and appropriate high-temperature design rules for devices that operate cyclically at high-temperatures where creep is not negligible.

Dimensional instabilities due to possible void swelling and irradiation creep has also not received sufficient attention, particularly when the perturbing effects of He and H are considered. While the incubation period for onset of swelling in RAF/M steels is believed to be quite long this may not be the case when He and H are produced concurrently with displacement damage.

Finally, development and qualification of fabrication and joining technologies for TBMs along with appropriate NDE techniques and procedures is beginning to receive considerable attention as the opportunity for testing advanced blanket concepts in ITER draws nearer. The exact level of effort to license a TBM for service in ITER is not known, but because these modules are geometrically complex, involve many dissimilar materials, and will utilize a relatively large number of fabrication and joining methods that have not been nuclear qualified, it is anticipated that significant work remains to be done.

Acknowledgments

This work was performed, in part, under the auspices of the US Department of Energy, Office of Fusion Energy Sciences, under Contract DE-AC06-76RLO1830.

References

[1] S. Jitsukawa, A. Kimura, A. Kohyama, et al., J. Nucl. Mater. 329–333 (2004) 39.
[2] N. Baluc, D.S. Gelles, S. Jitsukawa, et al., J. Nucl. Mater. 367–370 (2007) 33.
[3] N. Baluc, K. Abe, J.L. Boutard, et al., Nucl. Fusion 47 (2007) S696.
[4] T. Yamamoto, G.R. Odette, H. Kishimoto, et al., J. Nucl. Mater. 356 (2006) 27.
[5] E. Lucon, W. Vandermeulen, J. Nucl. Mater., these Proceedings.
[6] E. Lucon, W. Vandermeulen, SCK•CEN Open Report BLG-1042 Rev. (1) (2007).
[7] B. van der Schaaf, C. Petersen, Y. de Carlan, J.W. Rensman, E. Gaganidze, X. Averty, J. Nucl. Mater. 386–388 (2009) 236.
[8] J.-W. Rensman, J. Nucl. Mater., these Proceedings.
[9] P. Spätig, R. Stoenescu, P. Mueller, et al., J. Nucl. Mater., these Proceedings.
[10] A.D. Whapman, M.J. Makin, Phil. Mag. 5 (1960) 237.
[11] G.R. Odette, T. Yamamoto, H.J. Rathbun, et al., J. Nucl. Mater. 323 (2003) 313.
[12] G.R. Odette, M.Y. He, T. Yamamoto, J. Nucl. Mater. 367–370 (2007) 561.
[13] P. Mueller, P. Spätig, R. Bonadé, et al., J. Nucl. Mater., these Proceedings.
[14] R.L. Klueh, M.A. Sokolov, K. Shiba, J. Nucl. Mater., these Proceedings.
[15] M.A. Sokolov, H. Tanigawa, G.R. Odette, et al., J. Nucl. Mater. 367–370 (2007) 68.
[16] H. Schroeder, P. Batfalsky, J. Nucl. Mater. 117 (1983) 287.
[17] R.L. Klueh, N. Hashimoto, M.A. Sokolov, et al., J. Nucl. Mater. 357 (2006) 156.
[18] R.L. Klueh, N. Hashimoto, M.A. Sokolov, et al., J. Nucl. Mater. 357 (2006) 169.
[19] R.J. Kurtz, G.R. Odette, T. Yamamoto, et al., J. Nucl. Mater. 367–370 (2007) 417.
[20] C.C. Fu, F. Willaime, Phys. Rev. B 72 (2005) 064117.
[21] T. Seletskaia, Y.N. Osetsky, R.E. Stoller, G.M. Stocks, Phys. Rev. Lett. 94 (2005) 046403.
[22] T. Seletskaia, Y.N. Osetsky, R.E. Stoller, G.M. Stocks, J. Nucl. Mat. 351 (2006) 109.
[23] K. Morishita, Phil. Mag. 87 (2007) 1139.
[24] L. Ventelon, B.D. Wirth, C. Domain, J. Nucl. Mat. 351 (2006) 119.
[25] H.L. Heinisch, F. Gao, R.J. Kurtz, J. Nucl. Mat. 367–370 (2007) 311.
[26] B.D. Wirth, G.R. Odette, J. Marian, et al., J. Nuc. Mater. 329–333 (2004) 103.
[27] V.A. Borodin, P.V. Vladimirov, J. Nuc. Mater. 362 (2007) 161.
[28] R. Schäublin, Y.L. Chiu, J. Nucl. Mater. 362 (2007) 152.
[29] G.R. Odette, M.J. Alinger, B.D. Wirth, Annu. Rev. Mater. Res. 38 (2008) 471.
[30] R. Lindau, A. Möslang, M. Rieth, et al., Fusion Eng. Design 75–79 (2005) 989.
[31] Y. de Carlan, M. Murugananth, T. Sourmail, H.K.D.H. Bhadeshia, J. Nucl. Mater. 329–333 (2004) 238.
[32] R.L. Klueh, N. Hashimoto, P.J. Maziasz, Scripta Mat. 53 (2005) 275.
[33] R.L. Klueh, unpublished research.
[34] S. Jitsukawa, F.W. Wiffen, R.E. Stoller, et al., J. Nucl. Mater., these Proceedings.
[35] A.-A.F. Tavassoli, A. Alamo, L. Bedel, et al., J. Nucl. Mater. 329–333 (2004) 257.
[36] L. Giancarli, V. Chuyanov, M. Abdou, et al., J. Nucl. Mater. 367–370 (2007) 1271.
[37] J.-F. Salavy, L.V. Boccaccini, G. De Dinechina et al., J. Nucl. Mater., these Proceedings.
[38] J. Aktaa, M. Weick, C. Petersen, J. Nucl. Mater., these Proceedings.
[39] B. Fournier, M. Sauzay, C. Caës, et al., Int. J. Fatigue 30 (2008) 649.
[40] B. Fournier, M. Sauzay, C. Caës, et al., Int. J. Fatigue 30 (2008) 663.
[41] B. Fournier, M. Sauzay, C. Caës, et al., Int. J. Fatigue (2008), doi:10.1016/j.ijfatigue.2008.02.006.
[42] J.S. Dubey, H. Chilukuru, J.K. Chakravartty, et al., Mater. Sci. Eng. A 406 (2005) 152.
[43] A. Orlová, J. Bursík, K. Kucharová, V. Sklenicka, Mater. Sci. Eng. A 245 (1998) 39.
[44] V. Sklenicka, K. Kucharová, M. Svoboda, et al., Mater. Char. 51 (2003) 35.
[45] R. Sunyk, J. Aktaa, J. Nucl. Mater. 367–370 (2007) 1404.
[46] A. Cardella, E. Rigal, L. Bedel, et al., J. Nucl. Mater. 329–333 (2004) 133.
[47] S.H. Bush, J. Press. Vessel Tech. 110 (1988) 225.
[48] T.M. Gurieva, V.T. Pronyakin, J. Nucl. Mater. 233–237 (1996) 918.
[49] L. Jones, J.-P. Alfile, Ph. Aubert, et al., Fus. Eng. and Design 51&52 (2000) 985.
[50] M. Onozuka, J.-P. Alfile, Ph. Aubert, et al., Fus. Eng. and Design 55 (2001) 397.
[51] M. Merola, P. Chappuis, F. Escourbiac, et al., Fus. Eng. and Design 61&62 (2002) 141.
[52] K. Ioki, M. Akiba, P. Barabaschi, et al., J. Nucl. Mater. 329–333 (2004) 31.
[53] M. Onozuka, K. Kikuchi, A. Kirihigashi, et al., Fus. Eng. and Design 75–79 (2005) 595.